Experimental Study on Target Localization for DTMB-Based Passive Bistatic Radar

Jiachuan Qian[1,2(✉)], Haijie Li[3], and Huijie Zhu[1,2]

[1] Science and Technology on Communication Information Security Control Laboratory, Jiaxing 314033, China
jiachuanqian@sina.com
[2] The 36th Research Institute of China Electronics Technology Group Corporation, Jiaxing 314033, China
[3] Huaxin Consulting and Designing Institute Co., Ltd., Hangzhou, China

Abstract. This paper introduces the target localization experiment using the digital television terrestrial broadcasting (DTMB) signal. Firstly, the feasibility and advantages of DTMB signal as an external illumination source signal are analyzed. Then the ambiguity function of DTMB signal is analyzed, as well as its distance and Doppler resolution. ECA algorithm is introduced to suppress direct wave and multipath clutter. In order to obtain the positioning results of target, the array antenna is used as the direction-finding antenna to measure the azimuth angle of target. Finally, the target localization experiment based on DTMB signal is designed, and the localization information of target is determined by combining the actual position of TV Tower and receiver in two dimensions.

Keywords: DTMB · Passive radar · Clutter suppression · Direction-finding · Location

1 Introduction

The passive bistatic radar (PBR) [1] system uses a non-cooperative illumination source to detect targets within the coverage area. Now that the spectrum resources are very limited, how to use the electromagnetic spectrum resources in a complex environment to carry out the target location of external radiation sources is a new research hotspot. The PBR has many advantages over the traditional detection system. It does not need a large-volume transmitter, which reduces the cost. Moreover, it does not emit signals and has good concealment capabilities. And bistatic station layout has certain anti stealth ability. The non-cooperative illumination source is generally TV [2], broadcast [3] or base station signals [4], and the wide distribution of the signals ensures the feasibility of target localization.

Digital Television Terrestrial Multimedia Broadcasting (DTMB) is a digital television standard with independent intellectual property rights proposed by China in 2006. DTMB innovatively uses Time Domain Synchronous Orthogonal-Frequency Division Multiplexing (TDS-OFDM) [5] modulation technology. The pseudo-random sequence

X. Wang et al. (Eds.): AICON 2021, LNICST 396, pp. 201–211, 2021.
https://doi.org/10.1007/978-3-030-90196-7_18

is used in the signal frame head, and the frame synchronization sequence of time-domain orthogonal coding is periodically inserted in each OFDM guard interval. Under this system, the spectrum efficiency is increased by 10% compared with the European Digital Video Broadcasting-Terrestrial (DVB-T) [6] standard, and there is more than 20 dB synchronization protection gain. At the same time, it is convenient for reliable synchronization and channel estimation, and can be extended for base station identification and terminal location. Relevant literature analyzes the feasibility of DTMB as an external illumination source for target detection, and designs related experiments to verify it. Many studies [7–11] mainly focus on the direct wave and multipath suppression of the received signal and the subsequent Range-Doppler processing results. However, there are relatively few studies on the localization of the target in space.

Aiming at the problem of target location, the receiver is improved in this paper. Usually, the PBR system contains two receiving antennas, a reference antenna and a monitoring antenna, so that direct wave and multipath suppression can be performed at the receiving end. The array antenna is used as the target monitoring antenna in this paper. First, the extended cancellation algorithm (ECA) [12] is used to suppress the direct wave and multipath for each subarray. Then the results are processed by Range-Doppler with the reference antenna signal to obtain the correlation. And the correlation of each subarray is input as the direction signal to get the direction. Finally, according to the results of direction and distance, the motion trajectory of target is obtained by combining the actual position of TV Tower and receiving station.

2 DTMB Signal Ambiguity Function

Ambiguity function [13] is an important tool for signal research in radar systems, and it is also suitable for DTMB-Based PBR. The auto-ambiguity function describes the joint characteristics of the time-frequency domain of the signals, and can reflect the distance and Doppler resolution of the target. Its calculation formula is defined as:

$$|\chi(\tau, f_\mathrm{d})| = \left| \int_{-\infty}^{\infty} s(t)s^*(t+\tau)e^{-\mathrm{j}2\pi f_\mathrm{d} t}dt \right| \tag{1}$$

Where $s(t)$ represents DTMB signal; τ represents delay; f_d represents Doppler frequency.

The frame header form of the DTMB signal frame is shown in Fig. 1. The signal frame consists of 420 symbols and consists of a pre-synchronization sequence of length 82, a PN255 sequence and a post-synchronization sequence of length 83. Pre-synchronization and post-synchronization are defined as cyclic extensions of PN sequences. And the inserted frame header between each signal frame is the same. Therefore, when calculating its autocorrelation function, these repeated PN sequences will lead to the secondary peak of the ambiguity function.

In order to solve the above problems, the most direct method is to correlate the echo signal with the locally known PN sequence at the receiving end, find the frame head in the echo signal and remove it before Range-Doppler processing. However, for the actual environment considered in this paper, both the bistatic distance difference and Doppler frequency of the target are within the position of the secondary peak. Figure 2 shows

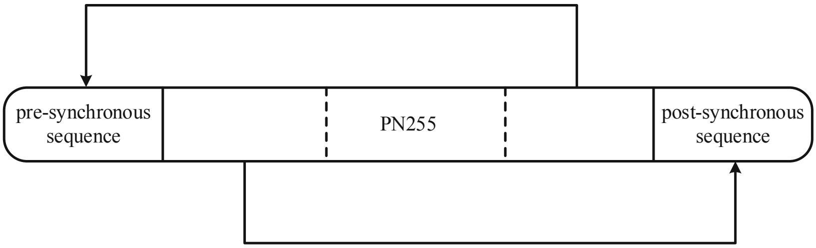

Fig. 1. DTMB signal frame header structure

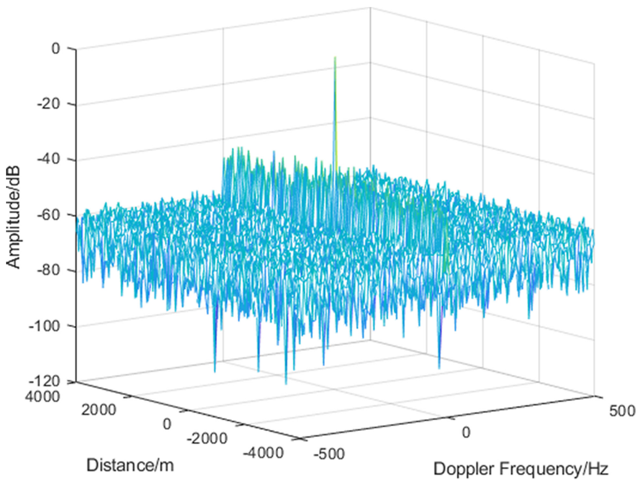

Fig. 2. The ambiguity function of the DTMB signal, where the bandwidth is 7.56 MHz, and the coherent integration time is 0.1 s.

the ambiguity function of the DTMB signal, where the bandwidth is 7.56 MHz, and the coherent integration time is 0.1 s.

The origin of the ambiguity function has a gain of about 40 dB compared to other points, showing an ideal pin shape. At the same time, the distance resolution is defined as:

$$\delta_d = \frac{c}{B} \tag{2}$$

Where c is the speed of light and B is the bandwidth of the signal. After calculation, the range resolution of the DTMB external radiation source radar is about 40 m. Therefore, DTMB signal is feasible as an external illumination source.

3 Key Technologies of DTMB-Based PBR

3.1 The Main Process of DTMB-Based PBR

Figure 3 shows the main flow of DTMB-Based PBR in this paper. There are two channels at the receiving end: monitoring channel and reference channel. The reference channel uses a high gain antenna to align with the direction of the TV tower to obtain the high signal-to-noise ratio (SNR) signal for subsequent processing. The monitoring channel uses an array antenna as the receiving antenna, aiming at the area to be detected, and the angle of arrival of the echo signal can be obtained. At the receiving end, the data is pre-processed to filter out other interfering signals. Then the reference signal of the reference channel is aligned with the echo signal of the monitoring channel in the time domain. Although the antenna of the monitoring channel is aimed at the area to be detected, a large number of direct waves and multipaths will mix into the reference channel in the complex urban environment, so the suppression of direct waves and multipath clutter is essential. Then perform range-Doppler processing between the suppressed residual signal and the reference signal, and extract the peak point. Each subarray can get peak points, and these points are used for interferometer direction-finding to obtain direction information. According to the actual positions of the TV Tower and the receiving station, the two-dimensional motion trajectory of the target is obtained by converting to the same coordinate system.

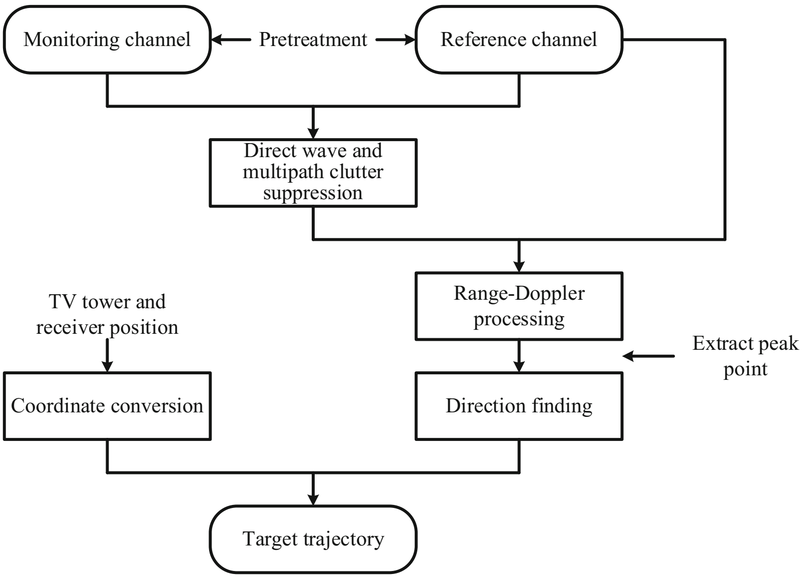

Fig. 3. The main flow of DTMB-Based PBR in this paper.

3.2 Direct Wave and Multipath Clutter Suppression

In the PBR system, the target echo signal is far lower than the direct wave and multipath clutter. Direct range-Doppler processing is not an ideal result, so the suppression of direct waves and multipath clutter is essential. Commonly used direct waves and clutter suppression include Least Mean Square (LMS) [14] algorithm, Recursive least squares (RLS) [15] algorithm and Extended Cancellation Algorithm (ECA) algorithm, etc. As an open-loop algorithm, ECA algorithm does not need iterative calculation, and the suppression effect is better. So, we choose ECA to deal with the problem in this paper. The main idea of ECA algorithm is that the reference signal and its time delay constitute a subspace, and calculate the projection coefficient of the echo signal on this subspace. Because of the Doppler frequency between the target and the clutter, it is usually considered that the target echo signal and the clutter are uncorrelated. Therefore, when the echo signal subtracts the reference signal and the subspace weighting composed of its delay, the echo target signal in the echo signal is considered to be unaffected, while the direct wave and multipath clutter are suppressed.

The antenna of the reference channel is aligned with the TV tower to sample and the reference signal is recorded as *ref*. The echo signal obtained by the monitoring channel aiming at the target area to be detected is denoted as *s*. The echo signal includes the direct signal of the TV tower, the multipath signal of the building, the reflection signal of the target and the noise. ECA algorithm is used to suppress the direct wave and multipath clutter in the echo, and the subspace composed of the reference signal and its delay can be expressed as:

$$\mathbf{V} = \begin{bmatrix} ref(1) & 0 & \cdots & 0 \\ ref(2) & ref(1) & \cdots & 0 \\ \vdots & \vdots & \vdots & \vdots \\ ref(L) & ref(L-1) & \cdots & ref(L-K) \end{bmatrix} \tag{3}$$

Where L represents the length of the signal, and K represents the order of canceling multipath clutter.

Finding the projection coefficient of the echo signal in the subspace is a convex optimization problem:

$$w = \arg\min_{w} \|s - \mathbf{V}w\|_2^2 \tag{4}$$

The gradient of the objective function is obtained by deriving w in the above formula. Let the gradient be 0, that is:

$$\frac{\partial(\|s - \mathbf{V}w\|_2^2)}{\partial w} = 0 \tag{5}$$

We can get the weight vector:

$$w = (\mathbf{V}^H\mathbf{V})^{-1}\mathbf{V}^H s \tag{6}$$

The residual signal after clutter suppression can be obtained by subtracting the product of the sliding matrix and the weight vector from the echo signal. It can be expressed as:

$$echo = s - \mathbf{V}w = s - \mathbf{V}(\mathbf{V}^H\mathbf{V})^{-1}\mathbf{V}^H s \tag{7}$$

The accuracy of the weight vector obtained by ECA is related to the data length and K value of the signal. The smaller the K is, the less obvious the effect of multipath elimination is. However, the larger the K is, the larger the computation will be. So, in data processing, the appropriate K is determined by considering the influence of multipath in the environment.

3.3 Direction-Finding Algorithm

The target echo signal is still weak, and the noise in the echo signal is still greater than the target echo signal after clutter suppression. It is necessary to perform Range-Doppler processing to improve the SNR of the signal. The calculation formula can be expressed as:

$$|\chi(\tau, f_{\mathrm{d}})| = \left| \int_0^T echo(t) s^*(t+\tau) e^{-\mathrm{j}2\pi f_{\mathrm{d}} t} dt \right| \tag{8}$$

After Range-Doppler processing, the peak point $(\tau_{\mathrm{m}}, f_{\mathrm{dm}})$ can be searched as the corresponding target information. So far, we get the speed and distance information of the target. However, there is still a lack of direction information to locate the target, which needs further processing to get the direction-finding results of the array antenna.

The essence of interferometer [16] direction-finding is to use the phase difference formed by the radiation signal on the receiving antenna to determine the direction of the signal. Based on the phase received by element 1 in the M-element antenna array, the phase difference between element M and reference element can be expressed as $\varphi(m - 1)$ (see Fig. 4).

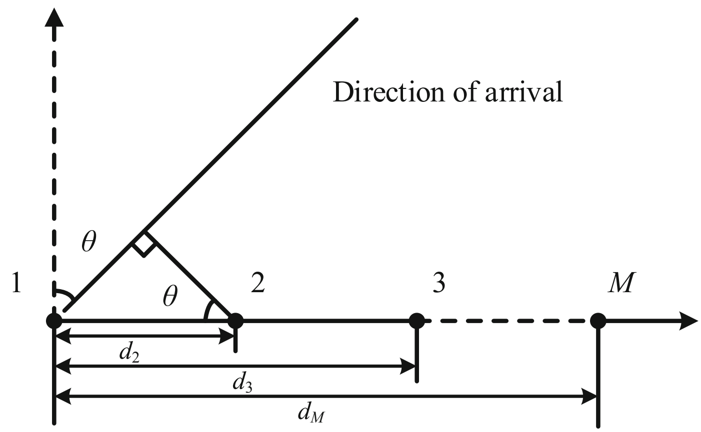

Fig. 4. Principle of interferometer direction-finding.

Where $m = 2,3\ldots M$ can form a phase difference vector $\boldsymbol{\varphi} = [\varphi(1), \varphi(2),\ldots, \varphi(M-1)]$. According to the geometric relationship of the linear array, the relationship between the phase and the direction of arrival can be obtained:

$$\varphi(m-1) = \frac{2\pi \cdot d_{m-1}}{\lambda} \sin\theta \tag{9}$$

Where d_m represents the distance between the m-th subarray and the (m + 1)-th subarray.

If the azimuth θ traverses 2π at a certain step angle, several pairs of the above-mentioned corresponding relations can be expressed as $\boldsymbol{u}(\theta,\varphi)$. The phase difference vector φ corresponding to these azimuth θ is the original phase difference sample. Correlation processing is the process of matching the observation samples generated by the signal response received by the array antenna with the standard samples. Therefore, the cost function of interferometer direction-finding can be expressed as:

$$F(\theta, \boldsymbol{\varphi}) = \frac{\boldsymbol{v}^{\mathrm{T}}\boldsymbol{u}(\theta, \boldsymbol{\varphi})}{\sqrt{(\boldsymbol{v}^{\mathrm{T}}\boldsymbol{v})}\sqrt{\boldsymbol{u}^{\mathrm{T}}(\theta, \boldsymbol{\varphi})\boldsymbol{u}(\theta, \boldsymbol{\varphi})}} \tag{10}$$

Where $\boldsymbol{v}$ represents the observed phase difference vector of the actual antenna.

In the actual environment, even if the ECA algorithm suppresses most of the direct wave and multipath clutter, the residual clutter and noise are still larger than the target echo. If the residual signal is directly used to calculate the observed phase difference vector, there will be a large error. In this paper, the peak points obtained from the above Range-Doppler processing are used as the basis for observing the phase difference vector rather than the phase of the residual signal. In this way, not only the original phase of the echo signal can be preserved, but also the SNR can be improved.

4 Experiments and Results

The experiment was conducted on the top of a building with latitude and longitude of (30.768933°, 120.73015°). Jiaxing DTMB TV Tower is located in the northeast of the building with latitude and longitude of (30.776908°, 120.741528°). NI USRP2955 is used as the acquisition device in the experiment, which adopts superheterodyne receiving system. It has a maximum instantaneous bandwidth of 80 MHz, 10 MHz–6 GHz RF tuning capability and four channel synchronous acquisition capability. In the experiment, the target is a flying unmanned aerial vehicle (UAV), its model is Dajiang mavic2, and its deployment size is 322 × 242 × 84 mm. The antenna for receiving the direct wave signal is facing the direction of the TV Tower, and its gain is about 15 dBi, which is connected with the collector channel 3. The linear array antenna used for direction-finding has three subarrays, and the distance are [0, 0.28, 0.7] m. It is connected to channel 0, channel 1 and channel 2 of the collector respectively, and the gain is about 7dBi. In the experiment, the linear array is placed in the same direction as the east-west direction, and the east direction is the positive direction of x-axis, and the north direction is the positive direction of y-axis.

The position of each point in the experimental scene is shown in Fig. 5 (ignoring the height information). The origin O is the location of the receiving antenna, and the P (x_0, y_0) point is the location of the TV Tower. The UAV flies in an east-west direction on the south side of the antenna, as shown by the line $y = -r$ in Fig. 5, and r is about 15m. Assuming that after data processing, we can get the bistatic distance difference $d = d_1 + d_2 - d_3$, and the angle θ, then the position of the UAV can be expressed as:

$$x = -\frac{d^2 + 2dd_3}{2d + 2d_3 + 2x_0 \sin\theta + 2y_0 \cos\theta} \sin\theta$$
$$y = -\frac{d^2 + 2dd_3}{2d + 2d_3 + 2x_0 \sin\theta + 2y_0 \cos\theta} \cos\theta \quad (11)$$

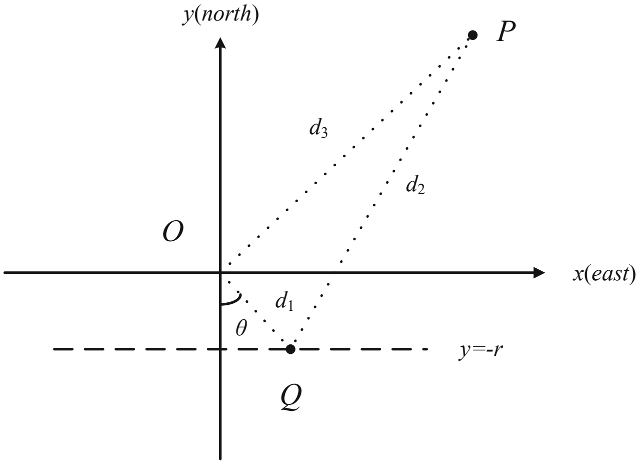

Fig. 5. Diagram of experimental scene.

In the data preprocessing part, the reference signal and the echo signal are aligned in the time domain (see Fig. 6). It can be seen that in urban environment, multipath effect is obvious, direct wave and multipath clutter suppression is essential.

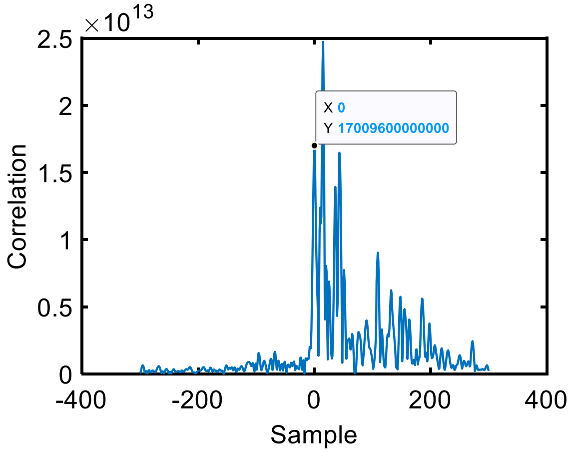

Fig. 6. Correlation of reference signal and echo signal in time domain.

Figure 7 shows the average power of each frame of echo signal in time domain before and after clutter suppression by ECA. It can be seen that most of the signals are suppressed.

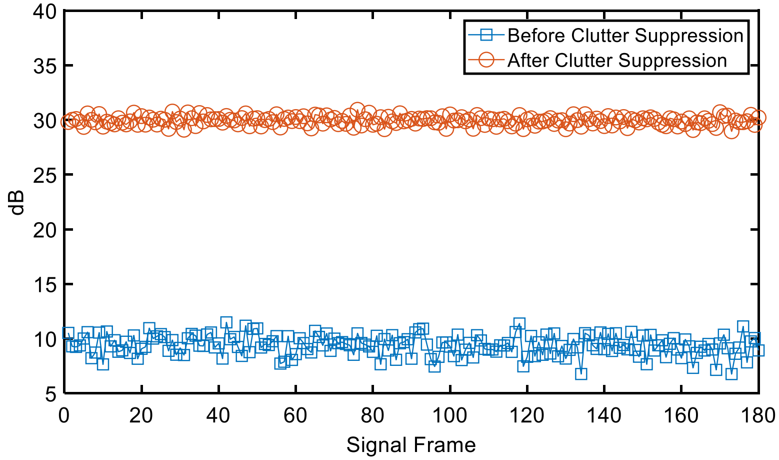

Fig. 7. The average power of each frame of echo signal in time domain before and after clutter suppression.

The distance and Doppler frequency information of UAV can be obtained by Range-Doppler processing of the residual signal and reference signal after suppressed, and the Coherent accumulation time is 100 ms. Figure 8 shows the Range-Doppler processing results of the three channels at a certain time. Because the distance between the subarrays is much smaller than the range resolution, the position of the peak point should be the same.

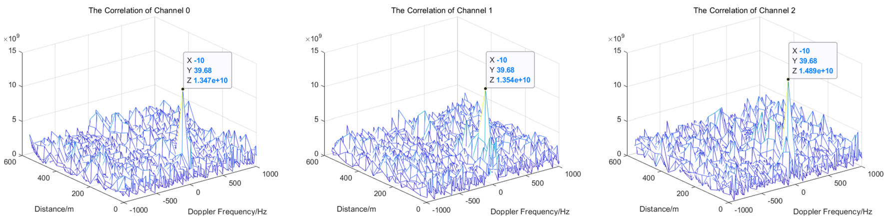

Fig. 8. Range-Doppler processing results of the three channels.

Extracting the peak value for the input of direction-finding of correlation interferometer. The direction-finding results in continuous time are shown in Fig. 9. And there is no obvious correlation peak in the position of −20°. This is because the bistatic range is the smallest at this time, and the Doppler frequency of the UAV changes positively and negatively, which leads to the increase of the correlation between the UAV echo signal and the reference signal, which is suppressed by ECA.

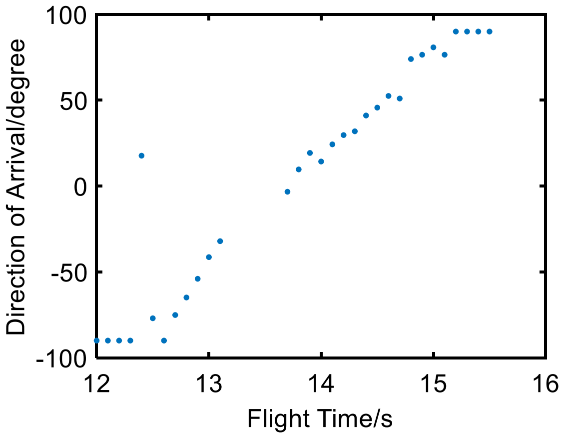

Fig. 9. Result of UAV direction-finding.

Substituting the results of direction finding and ranging into the above formula (11), the two-dimensional trace of the UAV in the x-y plane can be obtained (see Fig. 10). This shows that the UAV flies westward, and its trajectory is roughly the same as the actual scene. However, it is worth noting that the linear array used can only measure the azimuth without the pitch information, so the error caused by the altitude information is ignored. The error of linear array direction-finding results at the edge (±90°) is large.

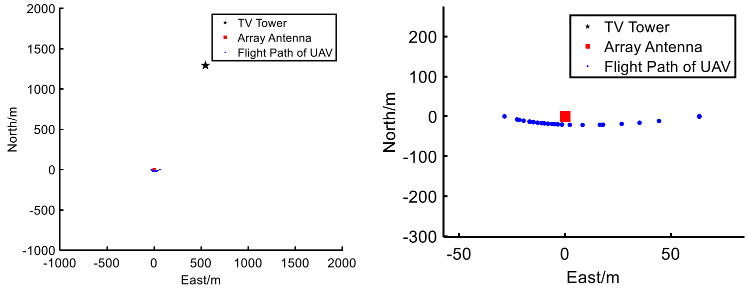

Fig. 10. UAV location experiment results

5 Conclusion

This paper briefly introduces the DTMB signal and analyzes its ambiguity function. In order to be able to be used for target location, the direct wave and multipath suppression algorithm and direction-finding algorithm are studied. On this basis, the UAV location experiment based on DTMB PBR is designed. After data processing, the flight trajectory of UAV in two-dimensional plane is obtained. Further research is carried out on how to further improve the positioning accuracy of UAV location.

References

1. Howland, P.E.: Target tracking using television-based bistatic radar. **146**(3), 166–174 (1999)
2. Griffiths, H.D., Long, N.R.W.: Television-based bistatic radar. IEE Proc. F-Commun. Radar Signal Process. **133**(7), 649–657 (2008)
3. Howland, P.E., Maksimiuk, D., Reitsma, G.: FM radio based bistatic radar. IEE Proc. Radar Sonar Navig. **152**(3), 107–115 (2005)
4. Tan, D., Lu, K.P., et al.: Passive radar using Global System for Mobile communication signal: theory, implementation and measurements. **152**(3), 116–123 (2005)
5. Wang, J., Yang, Z.X., Pan, C.Y., et al.: Iterative padding subtraction of the PN sequence for the TDS-OFDM over broadcast channels. IEEE Trans. Consum. Electron. **51**(4), 1148–1152 (2005)
6. Sun, Z., Wang, T., Jiang, T., et al.: Analysis of the properties of DVB-S signal for passive radar application. In: International Conference on Wireless Communications & Signal Processing, pp. 1–5. IEEE (2013)
7. Wan, X.R.: An overview on development of passive radar based on the low frequency band digital broadcasting and TV signals. J. Radars **1**(2), 109–123 (2012). (in Chinese)
8. Cardinali, R., Colone, F., Ferretti, C., et al.: Comparison of clutter and multipath cancellation techniques for passive radar. 469–474 (2007)
9. So, C.F., Ng, S.C., Leung, S.H.: RLS lattice algorithm using gradient based variable forgetting factor. In: IEEE, pp. 1168–117 (2003)
10. Ansari, F., Taban, M.R.: Implementation of sequential algorithm in batch processing for clutter and direct signal cancellation in passive bistatic radars. In: Electrical Engineering, pp. 1–6. IEEE (2013)
11. Meller, M.: Cheap cancellation of strong echoes for digital passive and noise radars. IEEE Trans. Signal Process. **60**(5), 2654–2659 (2012)
12. Colone, F., O'Hagan, D.W., Lombardo, P., et al.: A multistage processing algorithm for disturbance removal and target detection in passive bistatic radar. IEEE Trans. Aerosp. Electron. Syst. **45**(2), 698–722 (2009)
13. Saini, R., Cherniakov, M.: DTV signal ambiguity function analysis for radar application. **152**(3), 133–142 (2005)
14. Xu, Y.J., Tao, R., Wang, Y., et al.: Using LMS adaptive filter in direct wave cancellation. J. Beijing Inst. Technol. (Engl. Ed.) **12**(4), 425–428 (2003)
15. Dhiman, J., Ahmad, S., Gulia, K.: Comparison between Adaptive filter Algorithms (LMS, NLMS and RLS) (2013)
16. Lee, J.H., Woo, J.M.: Interferometer direction-finding system with improved df accuracy using two different array configurations. IEEE Antennas Wirel. Propag. Lett. **14**, 719–722 (2015)